Time-resolved fluorescence-line narrowing and energy-transfer studies in a Eu^{3+}-doped fluorophosphate glass

R. Balda and J. Fernández
Departamento de Física Aplicada I, Universidad del País Vasco, Alameda Urquijo s/n, 48013 Bilbao, Spain

J. L. Adam
Laboratoire de Verres et Céramiques, Campus de Beaulieu, Université de Rennes, 35042 Rennes, Cedex, France

M. A. Arriandiaga
Departamento de Física Aplicada II, Facultad de Ciencias, Universidad del País Vasco, Apartado 644, Bilbao, Spain
(Received 14 March 1996; revised manuscript received 16 May 1996)

The optical properties of Eu^{3+}-doped fluorophosphate glasses of composition (in mol %) 60 $NaPO_3$-15BaF_2-$(25-x)YF_3$-$xEuF_3$ ($x=0.5$, 2, 5, 10, 15, 20, and 25) have been investigated in the 4.2–300 K temperature range by using optical absorption spectroscopy and time-resolved resonant laser-induced fluorescence line narrowing. From the room-temperature absorption spectra Judd-Ofelt parameters have been obtained and used to calculate the spontaneous emission probabilities from the $^5D_0$ state. The spectral features of the time-resolved fluorescence line-narrowed $^5D_0 \rightarrow {}^7F_{0,1}$ emission spectra obtained under resonant excitation at different wavelengths along the $^7F_0 \rightarrow {}^5D_0$ transition as a function of concentration and temperature reveal the existence of energy migration between discrete regions of the inhomogeneous broadened spectral profile. From the concentration and time dependence of the average rate of excitation transfer, the electronic mechanism ruling the ion-ion interaction can be identified as a dipole-dipole energy transfer process. At low temperatures the average transfer rate parameter slightly depends on wavelength showing a temperature independent behavior. Above 77 K the weak dependence of the transfer rate on excitation wavelength (weak dependence on energy mismatch) together with its T^3 temperature dependence point to a transfer mechanism consistent with a two-site nonresonant two-phonon assisted process. The estimated average crystal field strength grows monotonically with the $^7F_0 \rightarrow {}^5D_0$ energy suggesting a large variation in the local environment of Eu^{3+} ions in these glasses. The slight increase with concentration of the $^5D_0$ fluorescence decays together with their single exponential character suggest that the transfer process may be fast enough to drive the system of excited centers to thermal equilibrium. [S0163-1829(96)06041-9]

I. INTRODUCTION

Rare earth (R) doped glasses have generated a great deal of interest as potential materials for optical devices in laser technology.[1] Among these materials, fluorophosphate glasses are promising host materials for optical applications because of their optical properties, low refractive indices, low dispersion, and good transparency from the ultraviolet to the infrared regions of the optical spectra.[2,3] In general, highly concentrated rare earth glasses are difficult to synthesize because they are very unstable materials. However, recently fluorophosphate glasses in the $NaPO_3$-BaF_2-RF_3 system have been obtained which are very stable and able to accept huge amounts of rare earth ions.[4] The optical properties of rare-earth ions in a glass material depend on the chemical composition of the glass matrix, which determines the structure and nature of the bonds.[5] The luminescence of local probes such as Eu^{3+} ions can provide an important information on the structure and properties of glasses. The optical properties of Eu^{3+} ions are well known to be highly sensitive to the local environment and have proved to be useful in the study of disordered media.[6–19] Since the first excited state $^5D_0$ is nondegenerate, the structure observed in the fluorescence spectra is only determined by the terminal ground state splittings. The inhomogeneous broadening of the $^7F_0 \rightarrow {}^5D_0$ absorption band is due to the site-to-site variations in the local field acting on the ions. However, the line can be narrowed by optical site-selective methods such as laser-induced fluorescence line narrowing (FLN). These techniques are useful in obtaining detailed information on the local field and ion-ion and ion-host interaction processes.

When the activator ion concentration in glass becomes high enough, ions interact by multipolar or exchange coupling, and ion-ion energy transfer occurs. Due to the inherent disorder of glass, ions in nearby sites may be in physically different environments with greatly varying spectroscopic properties. Therefore, besides causing a spatial migration of energy, transfer may also produce spectral diffusion within the inhomogeneously broadened spectral profile.[20]

There are several reasons why an understanding of energy transfer processes is of interest. From a technical point of view rare earth doped glasses are used nowadays in an extremely important class of optical devices including optical fiber amplifiers, lasers, light converters, sensors, etc. The development of more efficient rare earth materials for many of these devices requires a complete understanding of the processes which affect the optically excited state. From a more fundamental view, energy transfer processes involve physical phenomena which are the basis of more complex excitation transport in disordered solids.

Many experimental studies have been devoted to energy transfer in rare earth doped materials, but very few approach the fundamental interaction, probably because special pulsed laser sources and detection systems are required. Time-resolved fluorescence line-narrowing (TRFLN) techniques have only been used in a few studies on intraline energy transfer in glasses,[12,21–24] and among these, there is only one which analyses transfer process dynamics and its temperature dependence in Eu^{3+} doped calcium metaphosphate.[23] The knowledge about the temperature dependence of the transfer rate parameter in each particular system is of a great importance because it allows to determine the kind of mechanism involved in phonon assisted nonresonant energy transfer.

In a previous work some of the authors have investigated the spectral migration of the low temperature (4.2 K) time-resolved line-narrowed $^5D_0 \rightarrow {}^7F_0$ emission spectra of Eu^{3+} ions in $NaPO_3$-BaF_2-RF_3 fluorophosphate glasses. The results were found to be consistent with a dipole-dipole interaction mechanism among the Eu^{3+} ions.[25]

This work presents together with a detailed study of the optical properties of Eu^{3+} ions in fluorophosphate glasses of composition (in mol %) $60NaPO_3$-$15BaF_2$-$(25-x)YF_3$-x EuF_3 ($x=0.5$, 2, 5, 10, 15, 20, and 25) a dynamical study of the energy transfer mechanism in a broad temperature range between 4.2 and 200 K. The study includes absorption, Judd-Ofelt parameters calculations, lifetimes of the $^5D_0$ state, and time-resolved FLN of the $^5D_0 \rightarrow {}^7F_{0,1,2}$ resonant excited transitions, performed as a function of excitation wavelength and temperature. The spectral features of the time-resolved $^5D_0 \rightarrow {}^7F_{0,1}$ resonant excited spectra are analyzed in terms of phonon assisted energy transfer processes among the Eu^{3+} ions. From the temperature dependence of the transfer rate parameter two different phonon assisted mechanisms have been observed.

II. EXPERIMENT

The fluorophosphate glasses used in this study were prepared at the Laboratoire de Verres et Céramiques of the University of Rennes (France). Glasses were synthesized in the $NaPO_3$, BaF_2 (YF_3/EuF_3) system with the following compositions in mol %: $60NaPO_3$-$15BaF_2$-$(25-x)YF_3$-$xEuF_3$ ($x=0.5$, 2, 5, 10, 15, 20, 25), and designated as $NBEu_x$. Details on the entire glass forming diagram may be found in Ref. 4. Rare-earth oxides were processed by a fluorinating agent NH_4F, HF. The fluorination of the rare-earth oxides was carried out at 300 °C in a vitreous carbon crucible under argon atmosphere during four hours. Then, the excess of NH_4F, HF was eliminated at 800 °C, and the newly formed rare-earth fluoride was cooled down to room temperature. At this stage, the phosphate and fluorides were mixed together and the batch was heated up to 1100 °C for melting and refining for 15 min, then cooled down to 750 °C, and poured onto a brass mold preheated at the glass transition temperature, T_g. Finally, the samples were annealed at T_g before being appropriately cut and polished for the optical measurements.

The samples temperature was varied between 4.2 and 300 K with a continuous flow cryostat. Conventional absorption spectra were performed with a Cary 5 spectrophotometer. Resonant time-resolved fluorescence line-narrowed spectra were performed by exciting the samples with a pulsed frequency doubled Nd:YAG pumped tunable dye laser of 9 ns pulse width and 0.08 cm^{-1} linewidth and detected by a EGG-PAR optical multichannel analyzer.

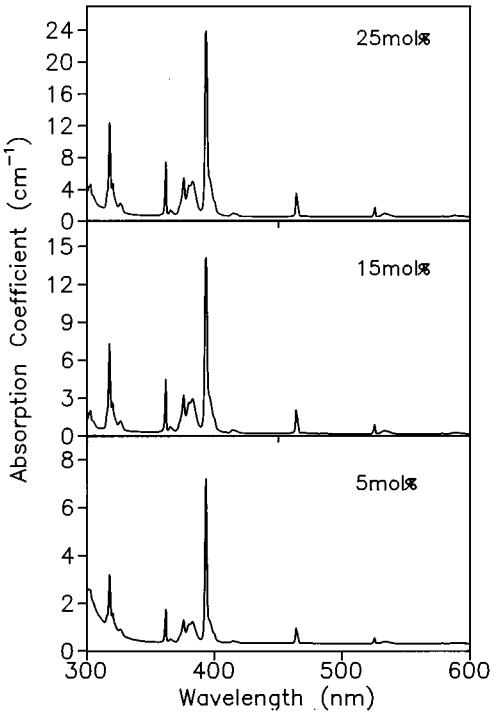

FIG. 1. Absorption spectra at room temperature of NBEu glass doped with three different concentrations: 5 mol % (bottom), 15 mol % (middle), and 25 mol % (top).

For lifetime measurements, the fluorescence was analyzed with a 1 m Spex monochromator, and the signal was detected by a Hamamatsu R928 photomultiplier. Data were processed by a boxcar integrator.

III. SPECTROSCOPIC RESULTS

A. Absorption properties

The room temperature absorption spectra were recorded for all samples in the 250–600 nm spectral range using a Cary 5 spectrophotometer. As an example Fig. 1 shows the room temperature absorption spectra of the glass doped with 5, 15, and 25 mol % of Eu^{3+} in the 300–600 nm range. The spectra consist of several inhomogeneously broadened transitions from the $^7F_0$ ground state and the thermally populated $^7F_1$ state to the excited states belonging to the $4f^6$ configuration.

Radiative emission probabilities of rare-earth ions can be determined by applying the Judd-Ofelt theory.[26,27] The method consists, first, in measuring the experimental oscillator strengths, f_{expt}, for every electronic transition arising from the ground state, $^7F_0$. However, in the case of Eu^{3+} ions, the first excited state, $^7F_1$, is thermalized at room temperature, so absorption occurs from that level as well. Thus experimental oscillator strengths were determined by means of the following equation:

$$f_{\text{expt}} = \frac{mc}{\pi e^2 N} \int \alpha(\nu) d\nu, \tag{1}$$

TABLE I. Measured and calculated (effective) oscillator strengths of Eu^{3+} ions in $NBEu_{15}$ fluorophosphate glass. Transitions are from the $(^7F_0, ^7F_1)$ states to the levels indicated. Wavelengths correspond to average transition energies. $\Omega_2=3.24$, $\Omega_4=5.11$, $\Omega_6=2.89$ (in 10^{-20} cm^2 units); $\delta_{rms}=8\times10^{-8}$.

Levels	Wavelengths (nm)	f_{expt} (10^{-8})	f_{calc} (10^{-8})	Residuals (10^{-8})
$^5D_1$	531.0	5	3	2
$^5D_2$	464.2	8	5	3
$^5D_3$	415.5	3	4	−1
$^5L_6$	394.5	105	108	−3
$^5G_2{}^5L_7$	380.0	88	92	−4
$^5G_{4,5,6}{}^5D_4$	362.4	17	15	2
$^5H_{4,5,6,7}$	319.6	98	94	4
$^5(I,H)_5{}^5F_{2,3,4,5}{}^5I_4$	298.0	85	86	−1
$^5(I,H)_6{}^5I_7$	286.0	38	21	17

where the integrated absorption coefficient is computed for transitions from $(^7F_0, ^7F_1)$ (m and e are the electron mass and charge, c the light velocity, and N is the number of active species per cm^3) which was 2.41×10^{21} ions cm^{-3} for the $NBEu_{15}$ sample used to calculate the Judd-Ofelt parameters.

According to the theory, the expression for the calculated oscillator strength (f_{calc}) for a $SLJ\rightarrow S'L'J'$ transition is

$$f_{calc}(J,J') = \frac{8\pi^2 m\overline{\nu}}{3h(2J+1)e^2n^2} \times[\chi_{ed}S_{ed}(J,J') + \chi_{md}S_{md}(J,J')], \quad (2)$$

where $\overline{\nu}$ is the average frequency of the transition and h is the Planck constant. A constant value of 1.518 was used for n, the refractive index of the medium. The χ factors, which correct for the effective field at an active center in the glass, are equal to $n(n^2+2)^2/9$ and n^3, for electric dipole (ed) and magnetic dipole (md) transitions, respectively. The electric dipole line strength, S_{ed}, is a function of the Judd-Ofelt parameters Ω_t and matrix elements $U^{(t)}$, with $t=2,4,6$, whereas S_{md} depends on the matrix elements of $(L+2S)$, as shown in Eqs. (3) and (4):

$$S_{ed}(J,J') = e^2 \sum_{t=2,4,6} \Omega_t(\langle f^N J||U^{(t)}||f^N J'\rangle)^2, \quad (3)$$

$$S_{md}(J,J') = \frac{e^2h^2}{16\pi^2m^2c^2}(\langle f^N J||\mathbf{L}+2\mathbf{S}||f^N J'\rangle)^2. \quad (4)$$

For Eu^{3+} ions, all absorption lines are assumed to be pure electric dipole in nature, including the weak $(^7F_0, ^7F_1 \rightarrow {}^5D_1)$ transition which is small enough to be neglected. Because thermalization occurs between the ground state and the first excited state at room temperature, we have defined an effective oscillator strength:

$$f_{eff} = \frac{(2J_0+1)f_0 + (2J_1+1)f_1e^{-\Delta E/kT}}{(2J_0+1)+(2J_1+1)e^{-\Delta E/kT}}, \quad (5)$$

where f_0 and f_1 refer to the calculated oscillator strength for $^7F_0$ and $^7F_1$, respectively. ΔE, the energy gap between these two levels, is estimated to be equal to 280 cm^{-1} from the absorption spectrum. k is the Boltzmann constant.

The intensity parameters Ω_t of Eq. (3) are found by a least-squares fitting of the experimental and effective electric dipole oscillator strengths. The results are shown in Table I.

It should be noted that the absorption bands permitted from the ground state to the $^7F_2$, $^7F_4$, $^7F_6$ levels were not included in the fitting procedure. The first one is simply beyond the multiphonon absorption edge of the glass. The second one overlaps with a strong absorption band located around 2200 cm^{-1}, due to the presence of phosphate groups. The third one is observed; however, this transition only depends on a $U^{(6)}$ matrix element ($U^{(2)}=U^{(4)}=0$) which is, in addition, two orders of magnitude higher than the other transition matrix elements. Thus in the present case, $^7F_0\rightarrow{}^7F_6$ acts as a hypersensitive transition and was deleted from the procedure.

The remaining absorption bands, located in the visible and ultraviolet (UV) regions, were assigned and their respective $U^{(t)}$ matrix elements attributed, according to the results by Carnall *et al.* for Eu^{3+} aquo ions.[28] It is well known that band positions and $U^{(t)}$ element values are quasi-host-independent. When several transitions overlap, which is often the case in the UV, an appropriate combination of these elements was used in Eq. (3).

Finally, an excellent fit was obtained between the experimental and calculated oscillator strengths, as indicated by the root-mean-square deviation, δ_{rms}, equal to 8×10^{-8}. This value favorably compares with results obtained for other ion-host combinations.[29,30] The phenomenological Judd-Ofelt parameters for Eu^{3+} ions in NBEu fluorophosphate glass are found to be $\Omega_2=3.24$, $\Omega_4=5.11$, $\Omega_6=2.89$, in 10^{-20} cm^2 units.

By means of these Ω_t parameters, the radiative emission probabilities can be calculated through the following equation:

$$A(J,J') = \frac{64\pi^4\nu^3}{3h(2J+1)c^3}[\chi_{ed}S_{ed}(J,J') + \chi_{md}S_{md}(J,J')]. \quad (6)$$

Also, one defines the radiative lifetime for a given excited state SLJ

TABLE II. Calculated spontaneous emission probabilities, radiative lifetime, and branching ratios for transitions from the $^5D_0$ level of Eu^{3+} ions in $NBEu_{15}$ fluorophosphate glass. (md) and (ed) stand for magnetic and electric dipole, respectively.

Transitions	λ (nm)	A (s^{-1})	τ_{rad} (ms)	β
$^5D_0 \rightarrow {}^7F_1$	590	51 (md)	4.2	0.22
$^5D_0 \rightarrow {}^7F_2$	609	104 (ed)		0.44
$^5D_0 \rightarrow {}^7F_4$	698	78 (ed)		0.33
$^5D_0 \rightarrow {}^7F_6$	802	2.5 (ed)		0.01

$$\tau_{rad} = \frac{1}{\sum_i A_i(J,J')} \tag{7}$$

and the branching ratio for a $SLJ \rightarrow S'L'J'$ transition

$$\beta(J,J') = \frac{A(J,J')}{\sum_i A_i(J,J')}, \tag{8}$$

where the summation is over all transitions from the excited state to the terminal levels. The results are given in Table II for transitions from the $^5D_0$ level to the ^7F_J levels ($J = 1,2,4,6$).

Transitions to $^7F_3$ and $^7F_5$ are forbidden:[28,31] $U^{(t)}=0$ and $\Delta J \neq 0, \pm 1$, whereas transitions to $^7F_2$, $^7F_4$, and $^7F_6$ are pure electric dipole ones. The $^5D_0 \rightarrow {}^7F_1$ transition, on the other hand, is magnetic-dipole allowed. It is well known that magnetic contributions depend on the χ_{md} factor only, the line strength being constant whatever the material. Thus, by means of data determined by Weber[32,33] for $YAlO_3$ crystals [$A_{md}(J,J')=107\ s^{-1}$ and $n_{c\ axis}=1.94$] we were able to determine the magnetic dipole probability of 51 s^{-1} shown in Table II. This value is consistent with results obtained for parent materials, e.g., A_{md} (J,J') is equal to 58 s^{-1} for $Ba(PO)_3$ glass and 66 s^{-1} for Ba-Zn-Lu fluoride glasses, respectively.[34,35]

Finally, the radiative lifetime is found to be equal to 4.2 ms for $^5D_0$, which is in good agreement, within 10%, with the experimental value of 3.8 ms measured for a 0.5% doped sample. This shows the validity of the Judd-Ofelt calculation for Eu^{3+} ions, provided that thermalization between the ground state and the first excited state is taken into account.

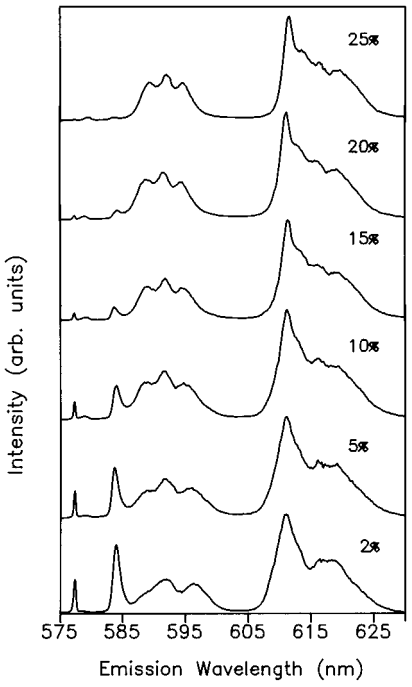

FIG. 2. Time-resolved line-narrowed emission spectra of $^5D_0 \rightarrow {}^7F_{0,1,2}$ transitions of Eu^{3+} ions in NBEu glass doped with 2, 5, 10, 15, 20, and 25 mol % of Eu^{3+} ions. The fluorescence was measured at 4.2 K at a time delay of 1 ms after the laser pulse and under excitation at 577.2 nm.

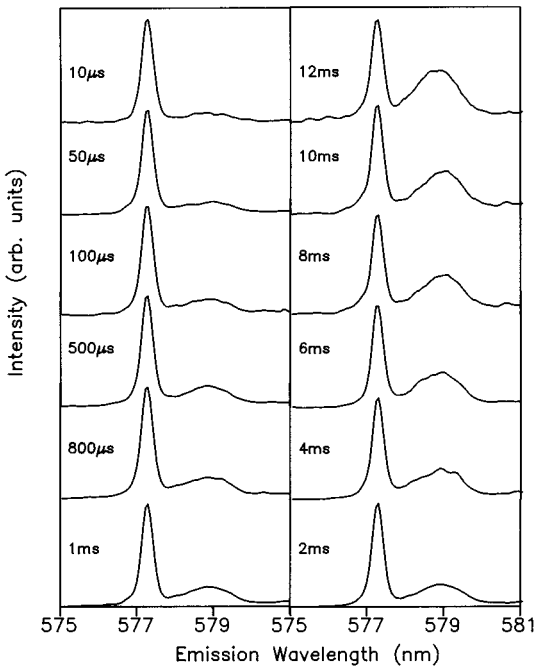

FIG. 3. Line-narrowed fluorescence spectra of the $^5D_0 \rightarrow {}^7F_0$ transition in NBEu glass doped with 10 mol % of Eu^{3+} obtained under excitation at 577.2 nm at different time delays after the laser pulse ranging from 10 μs to 12 ms. Measurements were performed at 4.2 K.

B. Time-resolved FLN studies

Time-resolved line-narrowed fluorescence spectra of the $^5D_0 \rightarrow {}^7F_{0,1,2}$ transitions of Eu^{3+} in $NBEu_x$ glasses were obtained between 4.2 and 200 K by using different resonant excitation wavelengths in the $^7F_0 \rightarrow {}^5D_0$ inhomogeneous absorption profile. These spectra were obtained at different time delays after the laser pulse. Figure 2 shows the spectra at 4.2 K for samples doped with 2, 5, 10, 15, 20, and 25 mol % of Eu^{3+} obtained at 1 ms after the laser pulse by exciting at the high energy side of the $^7F_0 \rightarrow {}^5D_0$ inhomogeneous absorption profile (577.2 nm).

1. $^5D_0 \rightarrow {}^7F_0$ emission spectra

At low concentrations and time delays, the $^5D_0 \rightarrow {}^7F_0$ spectra show a narrowed peak (effective linewidth around 11 cm^{-1}) that varies linearly with laser excitation wavelength. At concentrations equal or higher than 2 mol % and as time increases, besides the narrow line, a broad (nonselected) emission appears indicating the existence of energy transfer

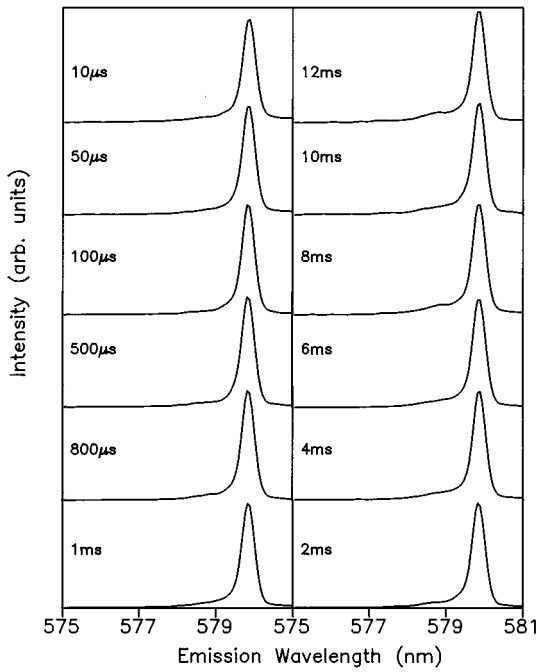

FIG. 4. Time-resolved line-narrowed fluorescence spectra of the $^5D_0 \rightarrow {}^7F_0$ transition in NBEu glass doped with 10 mol % of Eu^{3+} obtained under excitation at 579.8 nm at different time delays after the laser pulse ranging from 10 μs to 12 ms. Measurements were performed at 4.2 K.

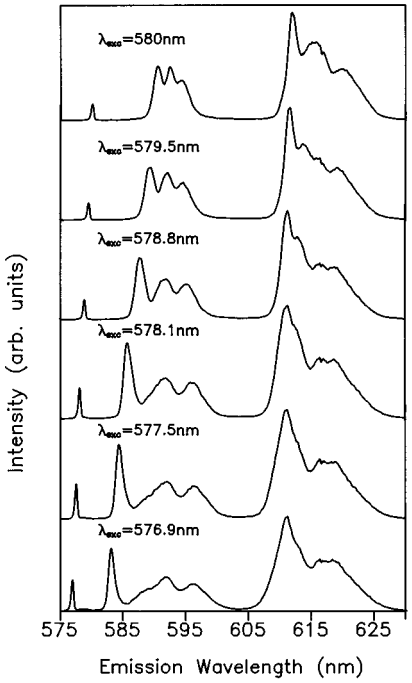

FIG. 5. Time-resolved line-narrowed emission spectra of $^5D_0 \rightarrow {}^7F_{0,1,2}$ transitions of Eu^{3+} ions in NBEu glass doped with 2 mol % of Eu^{3+} ions. The fluorescence was measured at 4.2 K at a time delay of 1 ms after the laser pulse and at different excitation wavelengths.

between discrete regions of the inhomogeneous broadened profile. Also as time increases, the relative intensity of both emissions changes, and the broad one becomes stronger. As an example, Fig. 3 shows the time evolution of the $^5D_0 \rightarrow {}^7F_0$ low temperature (4.2 K) emission spectra for the sample doped with 10 mol % of Eu^{3+}. The Eu^{3+} ions were excited on the high energy side of the inhomogeneous absorption band using a 577.2 nm laser pulse. At higher concentrations the transfer process appears at shorter time delays, but in all cases energy transfer produces a relative increase of the broad emission with respect to the narrow band (see Fig. 2 in Ref. 25).

The $^5D_0 \rightarrow {}^7F_0$ spectra were also performed by exciting at the low energy side of the inhomogeneous broadened absorption band as a function of time delay. Figure 4 shows the spectra for the sample doped with 10 mol % of Eu^{3+} obtained with a 579.8 nm laser pulse. The pattern of these spectra at 4.2 K reveals that the broad emission practically disappears, indicating that excitation energy can migrate mainly in one direction. Nevertheless, at temperatures higher than 40 K, the broad emission also appears on the high energy side of the narrow peak.

2. $^5D_0 \rightarrow {}^7F_1$ emission spectra

Figure 2 shows the time-resolved fluorescence-narrowed spectra of the $^5D_0 \rightarrow {}^7F_{0,1,2}$ emissions at 4.2 K obtained under resonant excitation at 577.2 nm within the $^7F_0 \rightarrow {}^5D_0$ inhomogeneous broadened absorption band for different concentrations. The spectra were obtained at a time delay of 1 ms. As can be observed, at a low concentration (2 mol %), $^5D_0 \rightarrow {}^7F_1$ transition shows three distinct main peaks due to the Stark splitting of the $^7F_1$ state, meaning that the Eu^{3+} ions are located in sites with C_{2v} symmetry or lower. However, for concentrations higher than 2 mol %, one additional peak appears beside the high energy component. As we shall see in the next section, this is due to the presence of phonon assisted energy transfer within the inhomogeneous broadened profile of a similar nature to the one present at the $^5D_0 \rightarrow {}^7F_0$ emission.

As was also observed for other glasses,[6,7,13,16–19] the Stark components of the $^7F_1$ multiplet noticeably differ in their evolution with excitation energy. The high energy (shortest wavelength) component is considerably sharper than the others and its location is more sensitive to the excitation energy. Figures 5 and 6 show the time-resolved emission spectra for samples doped with 2 and 10 mol % of Eu^{3+} ions at 4.2 K obtained under different resonant excitation wavelengths along the $^7F_0 \rightarrow {}^5D_0$ transition, and at 1 ms after the laser pulse. If compared with the $^7F_2$ multiplet, the evolution of the $^5D_0 \rightarrow {}^7F_1$ emission with the excitation wavelength is noticeable. As we mentioned before, besides the high energy $^7F_1$ Stark component of the $^5D_0 \rightarrow {}^7F_1$ emission (obtained by exciting at the high energy wing of the $^7F_0 \rightarrow {}^5D_0$ absorption band at 576.9 nm), Fig. 6 shows a bump at around 16 980 cm^{-1} which evolves with time and grows with concentration. In order to further investigate the origin of this additional emission peak in the $^5D_0 \rightarrow {}^7F_1$ transition, time-resolved emission spectra were performed under resonant excitation at the $^7F_0 \rightarrow {}^5D_0$ inhomogeneous broadened absorption band and at different time delays after the laser pulse ranging between 50 μs and 12 ms. As a first example, Fig. 7 shows the time-resolved spectra for a glass doped with 10 mol % of Eu^{3+} ions obtained under excitation at the high energy side

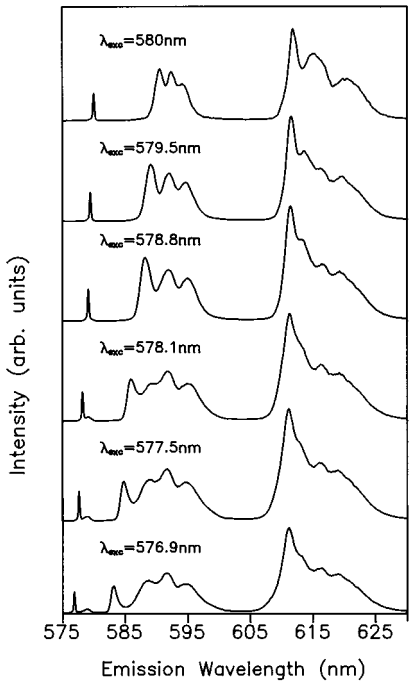

FIG. 6. Time-resolved line-narrowed emission spectra of $^5D_0 \rightarrow {}^7F_{0,1,2}$ transitions of Eu^{3+} ions in NBEu glass doped with 10 mol % of Eu^{3+} ions. The fluorescence was measured at 4.2 K at a time delay of 1 ms after the laser pulse and at different excitation wavelengths.

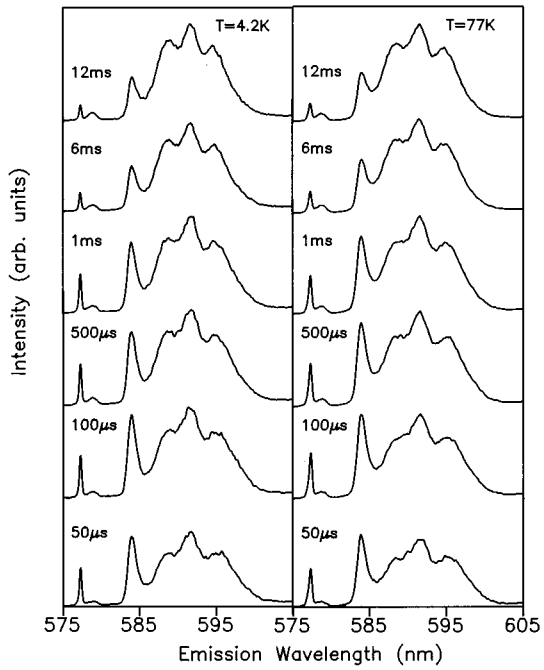

FIG. 7. Time-resolved line-narrowed emission spectra of $^5D_0 \rightarrow {}^7F_{0,1}$ transitions of Eu^{3+} ions in NBEu glass doped with 10 mol % of Eu^{3+} ions. The fluorescence was measured at 4.2 and 77 K, exciting at the high energy wing of the $^7F_0 \rightarrow {}^5D_0$ absorption band (577.2 nm) at different time delays after the laser pulse ranging between 50 μs and 12 ms.

of the $^7F_0 \rightarrow {}^5D_0$ transition (577.2 nm) at 4.2 K and at 77 K. As can be observed the high energy Stark component of the $^5D_0 \rightarrow {}^7F_1$ transition decreases as time increases at a rate similar to the one of the $^7D_0 \rightarrow {}^5F_0$ narrow peak, giving rise to a broad side band which is partially hidden by the other two enhanced Stark components.

As a second example, in Fig. 8 we present the time resolved site-selective emission spectra obtained under excitation at the low energy wing of the $^7F_0 \rightarrow {}^5D_0$ transition (579.8 nm) at 4.2 and 77 K, for time delays ranging between 50 μs and 12 ms. As can be seen, at helium temperature, and in accordance with the results obtained for the $^5D_0 \rightarrow {}^7F_0$ transition, transfer is negligible and the spectra mainly consist of three peaks. However, at 77 K and as time increases, besides the three peaks a shoulder appears on the high energy side of the first Stark component of the $^5D_0 \rightarrow {}^7F_1$ transition, the intensity of which grows stronger as time increases.

C. Lifetimes results

Lifetimes measurements performed at 77 K as a function of excitation wavelength, for samples doped with 2, 5, 10, 15, 20, and 25 mol % of Eu^{3+}, have shown that lifetimes remain nearly constant at wavelengths corresponding to the high energy side of the absorption band but then decrease as wavelength increases.[25] These measurements also showed a slight increase of the $^5D_0$ lifetime with Eu^{3+} concentration indicating the presence of transfer between europium ions. This fact, together with the single exponential character of the decays, suggests that the transfer process may be fast enough to drive the system of excited centers to thermal equilibrium. Another interesting feature is the wavelength dependence of lifetimes which shows a two-step behavior as excitation wavelength increases, supporting the existence of at least two broad varieties of Eu^{3+} field sites.

In this work lifetime measurements were obtained as a function of temperature and concentration. The decay times of the $^5D_0$ state were measured with a narrow band (0.08 cm^{-1}) tunable dye laser of 9 ns pulse width. The samples were excited at the $^7F_0 \rightarrow {}^5D_0$ transition and the luminescence collected at the high energy Stark component of the $^5D_0 \rightarrow {}^7F_2$ emission (612 nm). The observed decays remain single exponential at all temperatures and concentrations, which may be due to the use of narrow band laser excitation. As an example, Fig. 9 shows the room temperature logarithmic plot of the experimental decays for the samples doped with 5, 15, and 25 mol %, obtained by exciting at 578 nm.

Lifetime data as a function of concentration at 4.2 K, 77 K, and room temperature are shown in Fig. 10. As can be seen at concentrations higher than 20 mol %, lifetime decreases with temperature. Figure 11 shows this temperature dependence for the samples doped with 20, and 25 mol % in the 4.2–300 K range.

IV. DISCUSSION

A. $^5D_0 \rightarrow {}^7F_0$ emission spectra

The time evolution of laser-induced resonant line-narrowed fluorescence is produced by a combination of radiative decay and nonradiative transfer to other nearby ions. Subsequent fluorescence from the acceptors ions replicate the inhomogeneously broadened equilibrium emission profile, showing that transfer is not to resonant sites but to the

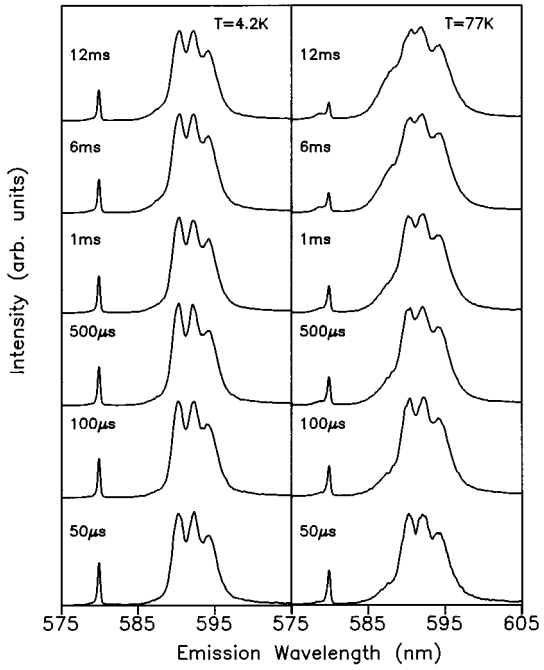

FIG. 8. Time-resolved site-selective emission spectra of $^5D_0 \rightarrow {}^7F_{0,1}$ transitions of Eu^{3+} ions in NBEu glass doped with 10 mol % of Eu^{3+} ions. The fluorescence was measured at 4.2 and 77 K exciting at the low energy wing of the $^7F_0 \rightarrow {}^5D_0$ absorption band (579.8 nm) at different time delays after the laser pulse ranging between 50 μs and 12 ms.

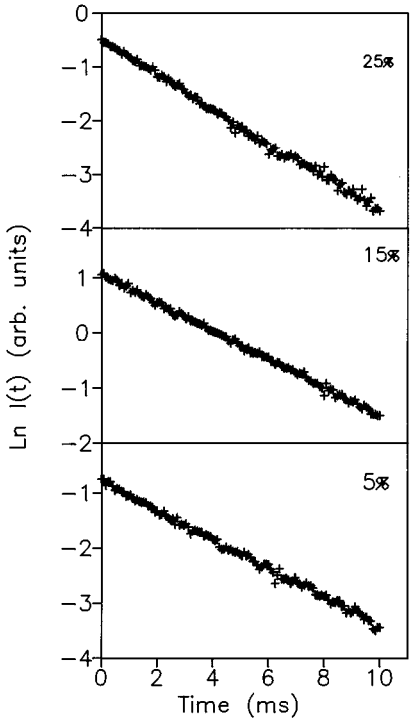

FIG. 9. Logarithmic plot of the fluorescence decays of the $^5D_0$ state for samples doped with 5, 15, and 25 mol % of Eu^{3+}. The decays were obtained by exciting at the $^7F_0 \rightarrow {}^5D_0$ absorption band (578 nm) and collecting at the first Stark component of the $^5D_0 \rightarrow {}^7F_2$ emission (610 nm). Measurements were performed at 295 K.

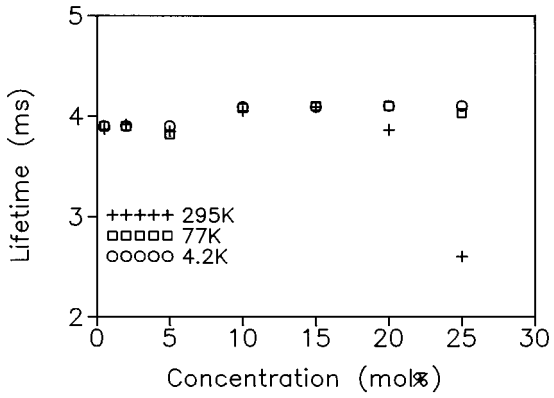

FIG. 10. Decay times obtained under excitation at 578 nm and collecting at the first Stark component of the $^5D_0 \rightarrow {}^7F_2$ emission (610 nm) as a function of Eu^{3+} concentration. Measurements are performed at 4.2, 77, and 295 K.

full range of sites within the inhomogeneous profile. In this case, a quantitative measure of the transfer is provided by the ratio of the intensity in the narrow line to the total intensity of the fluorescence in the inhomogeneous band.

One of the kinetic methods of migration investigation consists in analyzing time-resolved luminescence spectra after selective excitation.[24] As we have shown above at low temperature (4.2 K) the $^5D_0 \rightarrow {}^7F_0$ luminescence spectra reveal energy migration with increasing time delay only in the Stokes part of the inhomogeneous line shape. Neglecting the dispersion in the radiative decay rate, and using the Föster formula for dipole-dipole energy transfer, one can write for the relationship between the integral intensities of the broad background emission I_B, and the narrow luminescence component I_N,

$$\ln\left(\frac{I_B}{I_N}+1\right)=\gamma(E_L)t^{1/2}. \tag{9}$$

The macroscopic parameter $\gamma(E_L)$ has the meaning of an integral characteristic, reflecting the average rate of excitation transfer from donors to the ensemble of spectrally nonequivalent acceptors.[24]

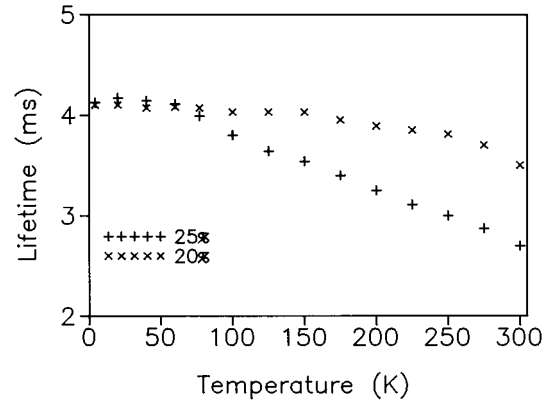

FIG. 11. Temperature dependence of the $^5D_0$ state lifetime of Eu^{3+} ions in glasses doped with 20 and 25 mol %. Lifetimes were obtained by exciting at 578 nm and collecting the fluorescence at the first Stark component of the $^5D_0 \rightarrow {}^7F_2$ emission (610 nm).

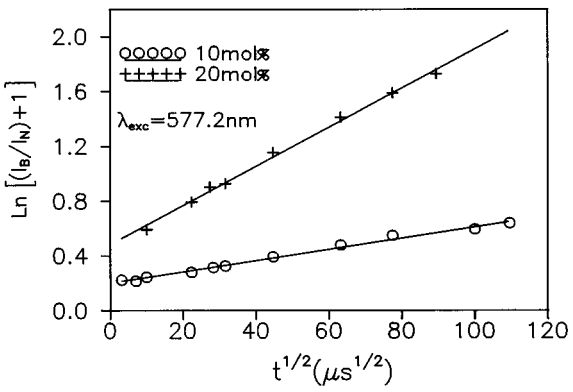

FIG. 12. Time evolution analysis of the $^5D_0 \rightarrow {}^7F_0$ luminescence spectra by means of Eq. (9) for samples doped with 10 and 20 mol % of Eu^{3+}. The spectra were obtained at different time delays after the laser pulse, between 10 μs and 12 ms, by exciting at the high energy wing of the $^7F_0 \rightarrow {}^5D_0$ transition (577.2 nm). Symbols (experimental data). Solid lines (fit). Data correspond to 77 K.

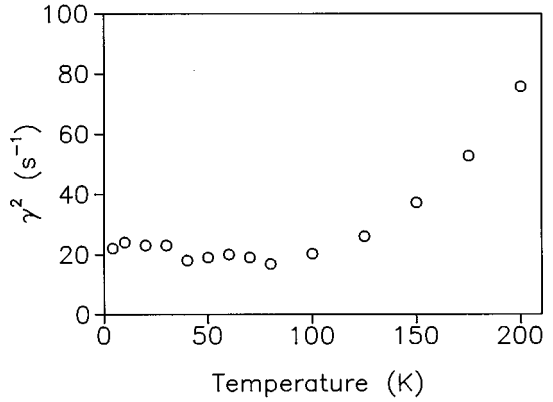

FIG. 13. Transfer rate as a function of temperature between 4.2 and 200 K for the sample doped with 10 mol % of Eu^{3+} ions. The transfer rate was obtained from the time resolved $^5D_0 \rightarrow {}^7F_0$ luminescence spectra measured by exciting at 577.2 nm at different time delays after the laser pulse from 10 μs to 12 ms.

We have analyzed the time-resolved site-selective fluorescence spectra of the $^5D_0 \rightarrow {}^7F_0$ transition obtained at different excitation wavelengths along the high energy side of the $^7F_0 \rightarrow {}^5D_0$ inhomogeneous absorption profile at different time delays between 10 μs and 12 ms according to Eq. (9). As an example, Fig. 12 shows the results for the samples doped with 10 and 20 mol % of Eu^{3+} at 77 K for an excitation wavelength of 577.2 nm. As can be observed a linear dependence of the $\ln(I_B/I_N+1)$ function on $t^{1/2}$ was found, indicating that a dipole-dipole mechanism of interaction among the Eu^{3+} ions dominates in this time regime. The same behavior was also observed in additional measurements at different temperatures and different excitation wavelengths. The small variation of the energy migration rate, $\gamma(E_L)$, with excitation wavelength suggests an energy mismatch (energy difference ΔE between nearby sites) independent mechanism. If this were the case, there are two possible mechanisms for the energy transfer:[36] one phonon assisted transfer or a two-site nonresonant process (involving one phonon action at each of two sites), which should show a linear and T^3 temperature dependence, respectively, being both independent of energy mismatch ΔE.

In order to further investigate the nature of the transfer mechanism we have measured the temperature dependence of the energy migration rate by analyzing the $^5D_0 \rightarrow {}^7F_0$ time-resolved spectra according to Eq. (9) between 4.2 and 200 K. The upper temperature limit was established because at temperatures higher than 200 K the $^5D_0 \rightarrow {}^7F_0$ spectra only show the broad component. The spectra were obtained by exciting at the high energy wing of the $^7F_0 \rightarrow {}^5D_0$ transition (577.2 nm). The dependence of the energy migration rate on temperature for the sample doped with 10 mol % of Eu^{3+} is shown in Fig. 13. As can be observed the transfer rate does not vary significantly between 4.2 and 77 K, but then increases with temperature. The transfer rate between 77 and 200 K closely follows a T^3 temperature dependence relationship as shown in Fig. 14.

The observed behavior, weak dependence of the transfer rate on excitation wavelength (weak dependence on the energy mismatch) together with a T^3 temperature dependence, is consistent with a two-site nonresonant process involving one phonon action at each of the two sites as has been shown by Holstein, Lyo, and Orbach.[36] This phonon assisted transfer process was previously observed in other Eu^{3+} doped glasses.[23] As far as concerns the low temperature behavior, the excitation wavelength dependence of the transfer rate was found to be slightly higher than at 77 K but nearly temperature independent as shown in Fig. 13. As pointed out in Ref. 24, this result is consistent with a mismatch dependent transfer process assisted by one acoustic phonon with the condition $kT \ll \Delta E$ and $\Delta E > 0$, where ΔE is the energy mismatch.

The concentration dependence of the spectral migration rate investigated from the FLN resonant spectra of samples with different concentrations obtained at 77 K and at 1 ms after the laser pulses,[25] further supports the dipolar nature of the ion-ion coupling mechanism.

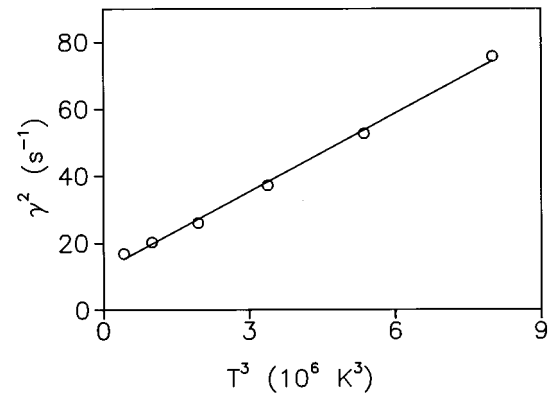

FIG. 14. Temperature dependence of the transfer rate between 77 and 200 K for the sample doped with 10 mol % of Eu^{3+} ions. The transfer rate was obtained from the time resolved $^5D_0 \rightarrow {}^7F_0$ luminescence spectra measured by exciting at 577.2 nm at different time delays after the laser pulse from 10 μs to 12 ms. Symbols (experimental data). Solid line (linear fit).

B. $^5D_0 \rightarrow {}^7F_1$ emission spectra

The nature of the energy transfer process can also be analyzed by means of the time-resolved site selective emission spectra for the $^5D_0 \rightarrow {}^7F_1$ transition. As we mentioned above, the $^5D_0 \rightarrow {}^7F_1$ emission shows more than the three peaks corresponding to the full Stark splitting of the $^7F_1$ level. Figure 7 shows the time resolved $^5D_0 \rightarrow {}^7F_1$ spectra for the sample doped with 10 mol % of Eu^{3+} ions obtained by exciting at the high energy wing of the $^7F_0 \rightarrow {}^5D_0$ transition. In this figure we can see that the intensity of the peak located around 16980 cm^{-1} increases with time delay, whereas the first Stark component intensity diminishes. Moreover, the linewidth of the first Stark component does not change significantly with increasing time delay in agreement with a nonresonant transfer process. As shown in the same figure, the spectral shape of this transition is similar at 4.2 and 77 K.

The $^5D_0 \rightarrow {}^7F_1$ time resolved spectra obtained under excitation at the low energy side of the $^7F_0 \rightarrow {}^5D_0$ transition at 77 K (see Fig. 8) also show a shoulder on the high energy side of the first Stark component which increases with time whereas the first component slightly decreases. However, at helium temperature, only the three peaks corresponding to the splitting of the $^7F_1$ level are observed. A similar behavior for this transition was found by Motegi and Shionoya[21] by studying energy migration among Eu^{3+} ions in a $Ca(PO_3)_2$ glass using time-resolved spectroscopy. The spectral features of the $^5D_0 \rightarrow {}^7F_1$ transition at 77 K were analyzed in terms of a phonon-assisted dipole-dipole process.

In our case, the spectral behavior of the first Stark component of the $^5D_0 \rightarrow {}^7F_1$ transition together with its associated peak is similar to the one observed for the $^5D_0 \rightarrow {}^7F_0$ emission. When excitation takes place at the high energy wing of the $^7F_0 \rightarrow {}^5D_0$ transition, at low temperature (4.2 K), the $^5D_0 \rightarrow {}^7F_1$ spectra reveal the existence of energy migration with increasing time delay in the Stokes part of the line shape. However under excitation at the low energy side of the $^7F_0 \rightarrow {}^5D_0$ transition the $^5D_0 \rightarrow {}^7F_1$ emission at 4.2 K only shows the three expected peaks and therefore no transfer occurs. In addition, as concentration rises there is also a parallel behavior between the time evolution of the narrow and background lines of the $^5D_0 \rightarrow {}^7F_0$ emission and the first Stark component and side band (bump) of the $^5D_0 \rightarrow {}^7F_1$ spectra. This parallelism between $^5D_0 \rightarrow {}^7F_0$ and $^5D_0 \rightarrow {}^7F_1$ spectral components is also present at different time delays, different excitation wavelengths, and different temperatures.

In order to confirm that the nature of the spectral kinetics within the $^5D_0 \rightarrow {}^7F_0$ and $^5D_0 \rightarrow {}^7F_1$ spectral components is the same, we have analyzed the time evolution of the relative intensity of the first component of the $^5D_0 \rightarrow {}^7F_1$ emission and its associated peak by making use of Eq. (9) as we did for the $^5D_0 \rightarrow {}^7F_0$ emission. In this case we have performed a Gaussian deconvolution of the $^5D_0 \rightarrow {}^7F_1$ spectra and calculated the intensity ratio of the first Stark component and its side broadband at different time delays ranging between 50 μs and 12 ms. As an example, Fig. 15 shows these results for the sample doped with 10 mol % of Eu^{3+} at 4.2 and 77 K for spectra obtained exciting at 577.2 nm (see Fig. 7). As can be seen the experimental points show a linear dependence on $t^{1/2}$. The γ values obtained from the slope of the straight lines are similar to those obtained for the $^5D_0 \rightarrow {}^7F_0$ emission.

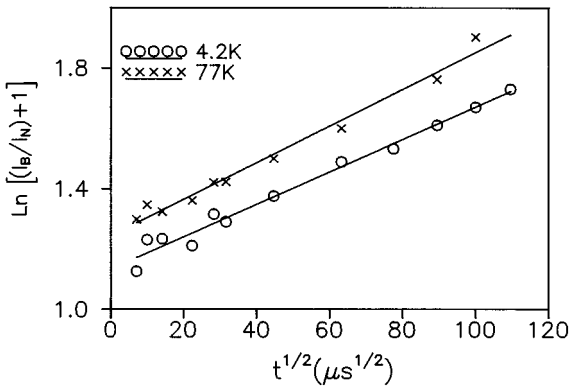

FIG. 15. Analysis of the time evolution of the first component and its side broadband in the $^5D_0 \rightarrow {}^7F_1$ luminescence spectra by means of Eq. (9) for the sample doped with 10 mol % of Eu^{3+}. The spectra were obtained at different time delays after the laser pulse between 50 μs and 12 ms by exciting at the high energy wing of the $^7F_0 \rightarrow {}^5D_0$ transition (577.2 nm). Symbols (experimental data). Solid lines (linear fit).

These features support the assumption of dipole-dipole phonon assisted energy transfer between $^5D_0$ states.

C. Estimation of the crystal field strength

As we have seen in the preceding experimental results, the time resolved emission spectra obtained under selective excitation along the $^7F_0 \rightarrow {}^5D_0$ transition show the variation of the $^7F_1$ splitting with respect to the $^7F_0 \rightarrow {}^5D_0$ energy. Although crystal field calculation is not the main purpose of

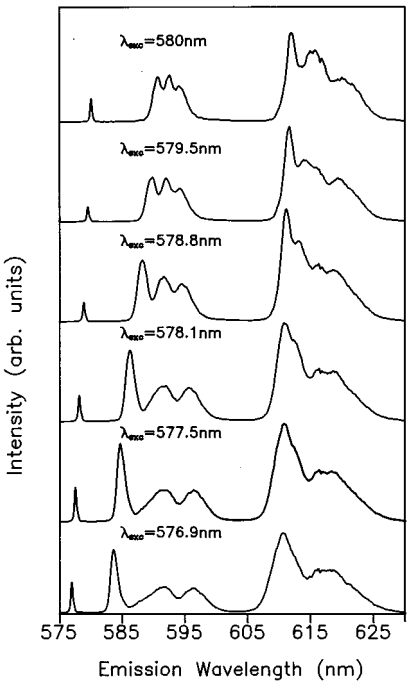

FIG. 16. Time-resolved line-narrowed emission spectra of $^5D_0 \rightarrow {}^7F_{0,1,2}$ transitions of Eu^{3+} ions in NBEu glass doped with 0.5 mol % of Eu^{3+} ions. The fluorescence was measured at 4.2 K at a time delay of 1 ms after the laser pulse and at different excitation wavelengths.

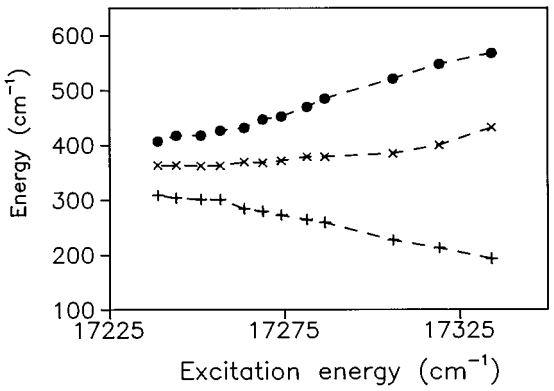

FIG. 17. Energy of the Stark components of the $^7F_1$ emission of Eu^{3+} in NBEu glass doped with 0.5 mol % of Eu^{3+} with respect to the $^7F_0 \rightarrow {}^5D_0$ excitation energy.

this work, we have used the time-resolved site-selective emission spectra as a function of excitation wavelengths along the $^7F_0 \rightarrow {}^5D_0$ absorption band to give an estimation of the crystal field strength. Figure 16 shows some of these spectra at 4.2 K for the sample doped with 0.5 mol % of Eu^{3+} ions. The average peak position energies of the three $^7F_1$ bands are plotted as a function of excitation energy in Fig. 17. In order to give a comparison between the crystal field (CF) strength in these compounds and other measured glasses, we have calculated the CF parameters (B_{kq}) assuming that in a first approximation the splitting of $^7F_1$ level depends on the $k=2$ terms of the second-order CF potential.[20] Defining an average CF parameter B_2 as $[(B_{20})^2+2(B_{22})^2]^{1/2}$, in Fig. 18 we present the variation of B_2 as a function of the $^7F_0 \rightarrow {}^5D_0$ energy calculated with the experimental data in Fig. 16. Figure 18 also shows for comparison other published values of B_2 in different glasses.[6,9,13,19] It is worthwhile noting that the average crystal parameter B_2 increases by a factor of three as $^7F_0 \rightarrow {}^5D_0$ ranges from low to high energy, therefore suggesting a large variation in the local environment of the Eu^{3+} ions in these

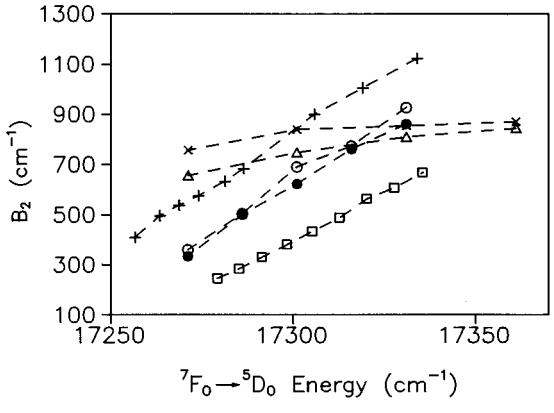

FIG. 18. Values of the B_2 parameter as a function of $^7F_0 \rightarrow {}^5D_0$ energy for some glasses. (+) corresponds to our experimental data; (○) and (●) represent data on ZBLAN and BIGaZYT fluoride glasses, respectively, from Ref. 19; (△) represents data on NaBaZn silicate glass from Ref. 6; (□) stands for data on KCaAl fluoroberillate glass from Ref. 9; and (×) stands for data on sodium aluminosilicate glass from Ref. 13.

glasses. This result is consistent with the assumption of phonon assisted energy transfer processes among Eu^{3+} ions mentioned above. Although the results in Fig. 18 suggest that the local environment of Eu^{3+} ions in this glass is similar to the one found in fluoride-type glasses some spectral features of the fluorescence emission show an intermediate behavior between a pure phosphate and a pure fluoride. The influence of glass composition on the emission spectra of Eu^{3+} can be described by the ratio of the $^5D_0 \rightarrow {}^7F_2$ and $^5D_0 \rightarrow {}^7F_1$ emission intensities which is related to the Judd-Ofelt parameter Ω_2. This parameter is related to the covalency and/or structural changes in the vicinity of Eu^{3+} ions.[38,34] In our case, according with a more covalent bonding character expected for the fluorophosphate glass, the ratio of the $(^5D_0 \rightarrow {}^7F_2)/(^5D_0 \rightarrow {}^7F_1)$ intensities gives a value of two which is higher than in pure fluoride glass[16] (around one) and in fluoroberilate glasses[9] where the $^5D_0 \rightarrow {}^7F_1$ emission is dominant. However, the observed lifetime of the $^5D_0$ state is closer to the one found in fluorides[12,16] which may indicate that the Eu^{3+} ion sites have a higher symmetry than in phosphate glasses. This combination of properties may be related with the mixed nearest-neighbor coordination as the influence of the local environment in the Eu^{3+} spectra not only depends on the geometrical changes of coordination but also on the nature of the coordinating species.

V. CONCLUSIONS

(i) From steady-state optical-absorption measurements, the Judd-Ofelt parameters were derived and used to calculate the radiative lifetime of the $^5D_0$ level.

(ii) Resonant time-resolved fluorescence line-narrowing spectroscopy shows the existence of energy migration between discrete regions of the inhomogeneous broadened $^5D_0$ spectral profile. The analysis of the $^5D_0 \rightarrow {}^7F_{0,1}$ emission spectra obtained as a function of time, concentration, and temperature shows that the electronic mechanism responsible for the Eu^{3+}-Eu^{3+} interaction is of the dipole-dipole type. At low temperatures the average transfer rate parameter slightly depends on wavelength, showing a temperature independent behavior. This result is consistent with a mismatch dependent transfer process assisted by one acoustic phonon. In the 77–200 K temperature range the weak dependence of the average transfer rate on excitation wavelength together with its T^3 temperature dependence indicates that energy transfer corresponds to a two-site nonresonant process involving one phonon action at each site. This crossover in the intraline transfer mechanism around 77 K points out to the necessity of more experimental investigations involving broad temperature ranges where different kinds of phonon assisted mechanisms may appear. Up to now, too few systems (crystals included[37]) have been studied in such a way so as to be able to conclude any general feature concerning the behavior of rare earths doped glasses.

(iii) The decays from the $^5D_0$ state were found to be single exponential for all temperatures and concentrations and their values slightly increase with concentration. This behavior suggests that the transfer process may be fast enough to drive the system of excited centers to thermal equilibrium. The wavelength dependence of lifetimes shows a two-step behavior as excitation wavelength increases

which supports the existence of at least two broad varieties of Eu^{3+} field sites.

(iv) In spite of the high concentrations of Eu^{3+} dopant attained in these glasses, the luminescence thermal quenching measured from the temperature dependence of lifetimes is small. This result could be very important for applications such as light converters, optical amplifiers and other optical devices.

(v) The strong increase of the average crystal parameter B_2 as a function of the $^7F_0 \rightarrow {}^5D_0$ energy suggests a large variation in the local environment for the Eu^{3+} ions in these glasses. Although this variation is similar to the one found in fluoride-type glasses, the spectral features of the $^5D_0 \rightarrow {}^7F_2$ emission show an intermediate behavior between a pure phosphate and a pure fluoride. This combination of properties can be understood by taking into account the mixed nearest-neighbor coordination, as the influence of the local environment in the Eu^{3+} spectra not only depends on the geometrical changes of coordination but also on the nature of the coordinating species.

ACKNOWLEDGMENTS

The authors wish to thank Angel J. García for spectra deconvolution. This work was supported by the Comision Interministerial de Ciencia y Tecnología (CICYT) of the Spanish Government (Ref. Mat93-0434), and Basque Country University (Ref. EB148/93 and Ref. EB034/95).

[1] M. J. Weber, J. Non-Cryst. Solids **123**, 208 (1990), and references therein.
[2] D. Ehrt and W. Seeber, J. Non-Cryst. Solids **129**, 19 (1991).
[3] M. J. Weber, C. Layne, R. Saroyan, and D. Milam, Opt. Commun. **18**, 171 (1976).
[4] M. Matecki, N. Duhamel, and J. Lucas, J. Non-Cryst. Solids **184**, 273 (1995).
[5] M. J. Weber, J. Non-Cryst. Solids **47**, 117 (1982).
[6] C. Brecher and L. A. Riseberg, Phys. Rev. B **13**, 81 (1976).
[7] J. Hegarty, W. M. Yen, and M. J. Weber, Phys. Rev. B **18**, 5816 (1978).
[8] J. Hegarty, W. M. Yen, M. J. Weber, and D. H. Blackburn, J. Lumin. **18/19**, 657 (1979).
[9] C. Brecher and L. A. Riseberg, Phys. Rev. B **13**, 2607 (1980).
[10] M. J. Weber and S. A. Brawer, J. Non-Cryst. Solids **52**, 321 (1982).
[11] X. Gang, G. Boulon, and R. C. Powell, J. Chem. Phys. **78**, 4374 (1983).
[12] X. Gang and R. C. Powell, J. Appl. Phys. **57**, 1299 (1985).
[13] J. A. Capobianco, T. F. Billeveau, G. Lord, and D. J. Simkin, Phys. Rev. B **34**, 4204 (1986).
[14] F. Durville, G. S. Dixon, and R. C. Powell, J. Lumin. **36**, 221 (1987).
[15] G. Nishimura and T. Kushida, Phys. Rev. B **37**, 9075 (1987).
[16] J. L. Adam, V. Ponçon, J. Lucas, and G. Boulon, J. Non-Cryst. Solids **91**, 191 (1987).
[17] J. Dexpert-Ghys, B. Piriou, N. Jacquet-Francillon, and C. Sombret, J. Non-Cryst. Solids **125**, 117 (1990).
[18] S. Todoroki, K. Hirao, and N. Soga, J. Appl. Phys. **72**, 5853 (1992).
[19] R. Balda, J. Fernández, H. Eilers, and W. M. Yen, J. Lumin. **59**, 81 (1994).
[20] M. J. Weber, in *Laser Spectroscopy of Solids*, edited by W. M. Yen and P. M. Selzer (Springer-Verlag, Berlin, 1981), p. 223, and references therein.
[21] N. Motegi and S. Shionoya, J. Lumin. **8**, 1 (1973).
[22] M. J. Weber, J. A. Paisner, S. S. Sussman, W. M. Yen, L. A. Riseberg, and C. Brecher, Phys. Rev. B **12/13**, 729 (1976).
[23] P. Avouris, A. Campion, and M. A. El-Sayed, Chem. Phys. Lett. **50**, 9 (1977).
[24] T. T. Basiev, V. A. Malyshev, and A. K. Przhevuskii, in *Spectroscopy of Solids Containing Rare-Earth Ions*, edited by A. A. Kapliansky and R. M. Macfarlane (North-Holland, Amsterdam, 1987), p. 303, and references therein.
[25] R. Balda, J. Fernández, N. Duhamel, J. L. Adam, and G. F. Imbusch, J. Lumin. **66&67**, 290 (1996).
[26] B. R. Judd, Phys. Rev. **127**, 750 (1962).
[27] G. S. Ofelt, J. Chem. Phys. **37**, 511 (1962).
[28] W. T. Carnall, P. R. Fields, and K. Rajnak, J. Chem. Phys. **49**, 4450 (1968).
[29] K. Tanimura, M. D. Shinn, W. A. Sibley, M. G. Drexhage, and R. N. Brown, Phys. Rev. B **30**, 2429 (1984).
[30] J. L. Adam, M. Matecki, H. L'Helgoualch, and B. Jacquier, Eur. J. Solid State Inorg. Chem. **31**, 337 (1994).
[31] R. Reisfeld, E. Greenberg, R. N. Brown, M. G. Drexhage, and C. K. Jørgensen, Chem. Phys. Lett. **95**, 91 (1983).
[32] M. J. Weber, T. E. Varitimos, and B. H. Matsinger, Phys. Rev. B **8**, 47 (1973).
[33] M. J. Weber, *Handbook of Laser Science and Technology* (CRC Press, Boca Raton, FL, 1982), Vol. 1.
[34] J. A. Capobianco, P. P. Proulx, M. Bettinelli, and F. Negrisolo, Phys. Rev. B **42**, 5936 (1990).
[35] G. J. Quarles, A. Suchocki, and R. C. Powell, J. Appl. Phys. **63**, 861 (1988).
[36] T. Holstein, S. K. Lyo, and R. Orbach, in *Laser Spectroscopy of Solids*, edited by W. M. Yen and P. M. Selzer (Springer-Verlag, Berlin, 1981), p. 40.
[37] W. M. Yen, in *Spectroscopy of Solids Containing Rare-Earth Ions*, edited by A. A. Kapliansky and R. M. Macfarlane (North-Holland, Amsterdam, 1987), p. 185.
[38] E. W. J. L. Oomen and A. M. A. van Dongen, J. Non-Cryst. Solids **111**, 205 (1989).